Effects Of Chemical Activation on Surface Sites of The Brick: pH-Dependence on Metal Adsorption

Oscar Allahdin, Belvia Bagoua, Michel Wartel, Joseph Mabingui, Abdel Boughriet

Abstract*—Brick was coated with ferrihydrite under variable experimental (pH) conditions. Pore – size distributions were determined and basic functions formed at brick surfaces were differentiated and quantified using pHmetry and conductimetry. Lead(II) and iron(II) adsorption capacities of synthesized compounds were tested by conducting fixed – bed column experiments. Both a higher pH used for Fe(III) precipitation into ferrihydrite and a higher level of deposited iron contributed to improve the adsorption performance of this material. The number of generated ΞAlO^-, ΞSiO^- and ΞFeO^- sites was found to be the key factor controlling the adsorption capacity level, and not physical and textural parameters.

Index Terms*—brick; ferrihydrite; pH; surface; adsorption; divalent metal.

I. INTRODUCTION

Lack of safe drinking water has become a worldwide problem, particularly, in developing countries. Thus, in poor rural regions of these countries, populations have often no access to clean and sanitized water supply, and hence, many (mostly children and elder people) died of severe waterborne deceases. To resolve that, development of water - treatment methods at low cost and high efficiency is necessary. Among these methods, adsorption has commonly been used for water purification, and different natural materials, mainly clay minerals, have been confirmed to be efficient adsorbents for the removal of heavy metals [1]. Moreover, according to Schwertmann and Cornell [2], iron oxides possess high affinity towards heavy metals and other toxic elements, and they can be used to adsorb metallic pollutants if they are deposited on to porous (natural) materials [3-8]. Our preliminary investigations revealed that the natural adsorption of raw brick (that can be considered roughly as a composite of sand and clays) made by craftsmen in Bangui region of Central African Republic, could be substantially increased if judiciously chosen chemical treatments (including hydrochloric leaching and ferrhydrite depositions) were adequately done [9-11].

In this work, Bangui brick grains were coated with ferrihydrite under variable experimental (pH) conditions, and basic functions generated at the surfaces of synthesized composites were differentiated and quantified using potentiometry and conductimetry. The effects of activation methods on the adsorption performance of coated brick in the removal of divalent metals (Fe^{2+} and Pb^{2+}) from water, was examined in terms of binding-sites concentration involved in the system. Lead(II) was chosen as adsorbate because of Pb poisoning effects/ environmental risks on water quality [12-14], and significant adverse influences on human health (particularly saturnisme), either through deficiency or toxicity [15]. Indeed, Pb accumulation within the body tends to be stored over time in the brain, bones, kidneys and the major organs; and Pb contamination results, even at low levels, in anemia, and subencephalopathic, neurological and behavioral effects on humans, particularly for children, and is also a strong threat during pregnancy [16-19]. Lead(II) - removal capabilities of different coated - brick samples were tested by conducting fixed-bed column experiments. Iron(II) was also chosen as adsorbate in the present work for the following reason. Most of ground waters in Bangui region contain high contents of Fe^{2+} ions that oxidize easily in contact with air oxygen into (colloidal) iron hydroxide. Ground waters then become no potable and in addition cannot be used for laundry because of its rust color. Iron(II) adsorption on coated brick and the possibility for the re-use of Fe(II)-doped brick once the column reached exhaustion were examined. Pore – size distributions of different coated - brick samples were also studied and their importance on the adsorption process was assessed.

Oscar Allahdin, Chaire Unesco "Sur la gestion de l'eau", Laboratoire Hydrosciences Lavoisier, Université de Bangui, Faculté des Sciences, BP. 908, République Centrafricaine

Belvia Bagoua, Chaire Unesco "Sur la gestion de l'eau", Laboratoire Hydrosciences Lavoisier, Université de Bangui, Faculté des Sciences, BP. 908, République Centrafricaine

Michel Wartel, Université Lille 1, Laboratoire LASIR (UMR CNRS 8516), Equipe Physico-chimie de l'Environnement. Bât. C8 2ème étage, 59655 Villeneuve d'Ascq cedex, France

Joseph Mabingui, Chaire Unesco "Sur la gestion de l'eau", Laboratoire Hydrosciences Lavoisier, Université de Bangui, Faculté des Sciences, BP. 908, République Centrafricaine

Abdel Boughriet, Université Lille 1, Laboratoire LASIR (UMR CNRS 8516), Equipe Physico-chimie de l'Environnement. Bât. C8 2ème étage, 59655 Villeneuve d'Ascq cedex, France

II. EXPERIMENTAL

A. Adsorbents preparation

The raw brick used in this study was obtained from Bangui region in the Central African Republic. Previously [9], X-ray diffraction and chemical analysis were performed on this material: ~ 61 wt % quartz; ~ 21 wt % metakaolinite; 3-4 wt % illite; $\leq$ 4 wt % iron oxides / hydroxides; and $\leq$ 2 wt % feldspar + mica + biotite. Before use, several physical / chemical treatments were carried out on the raw brick. First, it was broken into grains and sieved with sizes ranging from 0.7 to 1.0 mm. Second, the resulting particles were leached with a 6M HCl solution at 90°C for 3 hours. Third, a deposition of FeOOH onto HCl - treated brick was performed by a precipitation of iron(III) (by using a 0.25M Fe^{3+} ions solution) with NaOH solutions (6M and 1M) at different pH values ranging from 6.32 to 12.33.

B. Chemicals

All chemicals employed in the experiments were analytical grades. Sodium hydroxide and hydrochloride acid were supplied by DISLAB (France). The following salts: $Fe(NO_3)_3{\cdot}H_2O$ and $Pb(NO_3)_2$ were purchased from Prolabo, and $FeCl_2{\cdot}4H_2O$ from Merck.

C. ICP-AES analyses

All chemical attacks of brick materials were made with 2M nitric acid at 90°C for 2 hours. The recovered solutions were analyzed for metal contents using ICP-AES (Inductively Coupled Plasma - Atomic Emission Spectroscopy; model Varian Pro Axial View).

D. BET analyses

The physical characteristics (specific surface area, specific volume and pore size distribution) of coated brick were determined by the nitrogen adsorption isotherm (BET analysis) using Sorptomatic 1990 Carlo Erba at 77°K.

E. Fixed-bed column experiments

Continuous flow adsorption experiments were conducted in a fixed-bed glass column with an inner diameter of 12.5 mm, a height of 25 cm, and a 160-250µm porosity sintered-pyrex disk at its bottom in order to prevent any loss of material. A bed depth of 8.5 cm (10.0-10.5g) was investigated at a constant flow rate of 10 mL/min. Before being used in the experiments, at least ten bed volumes of Milli-Q water were passed through the column. The schematic diagram of the fixed-bed column reactor used is illustrated in Fig. 1.

1 : Pb(II) or Fe(II) solution
2 : Influent
3 : Glass column
4 : Brick pellets
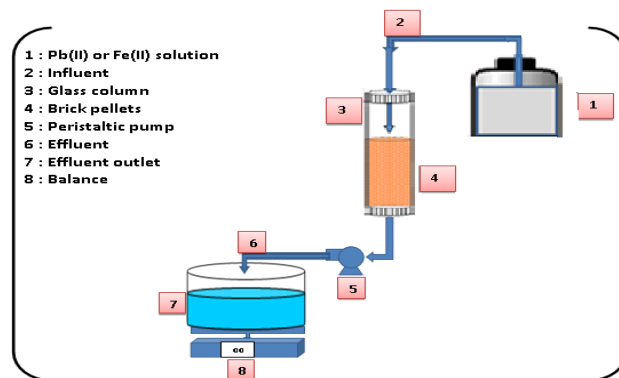5 : Peristaltic pump
6 : Effluent
7 : Effluent outlet
8 : Balance

Fig. 1: Schematic diagram of the fixed-bed column reactor used for metal adsorption on coated brick in water.

The initial concentration of metal cation (Fe^{2+} or Pb^{2+}) in the influent was 1.79×10^{-4} mole per liter. This content was chosen in this work because it generally represents an average level of soluble iron ($\approx$10 mg/L) found in ground waters from the Bangui region. The divalent - metal solution was pumped through the column at a desired flow rate by means of a peristaltic pump (Labo Moderne France Type KD1170) in a down-flow mode. During this column experiment, pH was measured, and effluent samples exiting the bottom of the column were collected at different time intervals and analyzed for metal contents using ICP-AES (Inductively Coupled Plasma - Atomic Emission Spectroscopy; model Varian Pro Axial View). Flow to the column continued until the effluent metal concentration at time t (C_t) reached the influent metal concentration (C_0): $C_t/C_0 \approx 0.99$. Performance of the packed bed was described in the present work using the concept of the breakthrough curve. After the exhaustion of coated brick by Pb^{2+} or Fe^{2+} ions, column was regenerated using a 150-mL NaClO solution (8g of chlorine per liter) at a flow rate of 5 mL/min in a down flow mode. The effluent solution was collected at periodically and analyzed for metal as given above. After elution, the column was rinsed with deionized water until the pH of wash water was approximately constant. The regenerated bed was again used for next cycle to explore the reusability of the brick.

F. pHmetric and conductimetric measurements

pHmetric and conductimetric titrations of coated brick samples, suspended in water, were performed using the Metrohm 888 Titrando autotitrator coupled to the 856 Conductimetry module. This system was equipped both with a combined Metrohm glass electrode (type 6.0262.100) and a Metrohm conductimetric Pt - cell (type 6.0915.100) with a cell constant of 0.69 cm^{-1}. The apparatus was connected to a PC, and automatic titrations were carried out using the Metrohm TIAMO 1.0 software in order to control titrant delivery, data acquisition and to check for potential stability. All measurements were conducted in a jacketed vessel at 25.0 $\pm$ 0.1 °C. Samples (0.5 g of coated brick in 90 mL of MilliQ water) were titrated with 0.05M HCl, under propeller stirring (by placing the propeller above brick grains in order to avoid their deterioration) and nitrogen stream to avoid CO_2 dissolution in the suspension. During analysis, increment 0.05-MHCl volumes of 1µL/sec were added to the

suspension if a potential variation < 2 mV/min and a conductance <10 mS/(cm.min), and the measurement was then made after an elapsed time of 1 min. These titrations could last up to one day. The pH and conductivity were measured simultaneously, and plotted automatically against added volume in real time owing to TIAMO software. These curves permitted to show transition point(s), confirming the presence of basic functions at the surface of coated brick grains.

III. RESULTS AND DISCUSSION

A. Effects of Fe(III)-precipitation pH on brick coating and Na content

Coated brick was synthesized at different Fe(III)-precipitation pH values ranging from 6.3 to 12.9, as described in the experimental section. A chemical attack with a 2M-HNO_3 solution was performed for 2 hours at 90°C on these coated - brick samples.

Overall, ICP-AES analysis of recovered solutions showed that: (i) no significant variations of iron contents were detected (see Fig. 2); and (ii) the amount of sodium varied weakly at pH < 7, then increased strongly up to pH ~ 11, and finally begin to decrease at pH > 12 (see Fig. 2).

These investigations allowed to evidence the relative importance of Fe(III) – precipitation pH in the fixation of Na atoms on the brick surface. Such bindings could be explained only by assuming the involvement of a NaOH - neutralization reaction implicating hydroxyl groups and leading subsequently to the generation of negatively charged sites on the brick.

The increase of negative charges at the brick surface (or Na^+ ions) should be an important factor in the performance of this material in its ability to remove cations from water. To check this, we tested in section III-B the lead(II) - adsorption properties of two coated - brick samples from column experiments: *one* prepared by precipitating Fe^{3+} ions at pH 6.3; and *the other* at pH 10.4.
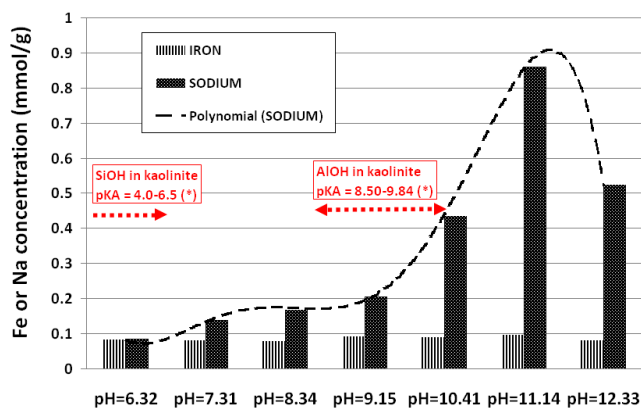
Fig. 2: Fe and Na contents (in mmol/g) determined by ICP-AES in coated – brick samples synthesized at Fe(III)-precipitation pH values ranging from 6.32 to 12.33. (*) see ref. 22.

In these compounds, Na contents determined by ICP-AES were found to be 0.085 and 0.434 mmole per gram of brick, respectively.

B. Lead(II) removal by coated brick in fixed – bed column

The effectiveness of two synthesized composites (at Fe(III)-precipitation pH values equal to 6.3 and 10.4) in the removal of Pb(II) ions was assessed under dynamic conditions using a fixed-bed column (as stated in the experimental section). The divalent-metal content in the column influent was fixed at 1.79×10^{-4} mol/L: this concentration corresponds to 37 ppm Pb. Results are presented graphically in Fig. 3.

As can be seen in this figure, an increase of Fe(III)-precipitation pH contributed to improve substantially Pb(II) removal from water. The breakthrough point was defined as the time, t, when the effluent concentration, C_t, attained $0.05 \times C_0$.
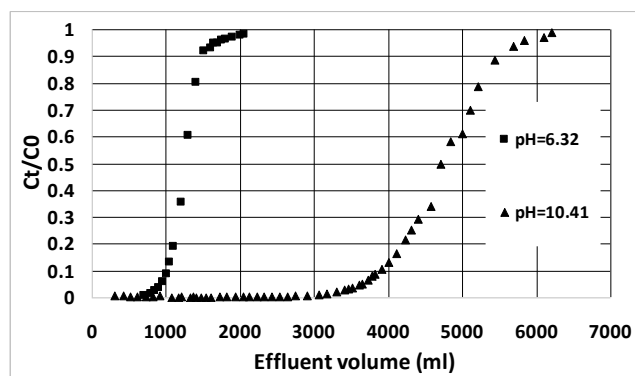
Fig. 3: Specific breakthrough curves of Pb(II) for a flow rate of 10 mL/min, a bed height of 8.5 cm (with an inside column diameter of 12.5 mm), and an influent concentration of 1.79×10^{-4} mole per liter. Adsorbents used: two coated - brick samples (with grains sizes ranging from 0.7 to 1.0 mm) were synthesized at Fe(III)-precipitation pH values equal to 6.3 and 10.4.

For these two fixed-bed column experiments, the corresponding effluent volume at breakthrough was found to be 900 and 3500 mL for composites prepared at Fe(III)-precipitation pH 6.3 and 10.4, respectively.

For a constant flow rate and at a given influent metal concentration, the total quantity of Pb^{2+} ions retained in the column (Q_{total}) was obtained graphically using Eqn. 1 by numerically integrating the area under the curve for adsorbed Pb(II) content (C_{ads}) versus time (t), where $C_{ads} = C_0 - C_t$ and C_0 is the influent metal concentration in mg/L.

$$Q_{total} = F \frac{A}{1000} = \frac{F}{1000} \int_{t=0}^{t=t_{total}} (C_{ads} dt) \qquad (1)$$

where F is the volumetric flow rate (mL/min); A is the area under the breakthrough (normalized) curve: C_t/C_0 vs. service time or effluent volume; t_{total} is the total flow time (min) necessary to observe the breakthrough phenomenon. In our studies, metal-adsorption capacity (in milligrams of adsorbed lead per 10 grams of brick pellets inside the column) was

found to be increased with an increase of Fe(III)-precipitation pH as follows: 44.6 mg at pH 6.3 and 164.6 mg at pH 10.4. However, it would be interesting to know the extent to which an increase of iron oxyhydroxide deposited on the brick at a controlled pH value could affect the adsorption performance of this material. On this view, we developed in the next section an easier method for coating brick, and at the same time, for increasing Fe content. For that, column experiments were performed by using 6M–HCl activated brick as starting adsorbent, Fe^{2+} ions as adsorbates, and a NaClO solution at pH 11 as the elution solution for column regeneration.

C. Effect of deposited iron content on the adsorption capacity of brick

The effectiveness of 6M-HCl activated brick in iron(II) removal was assessed under dynamic conditions using a fixed-bed column (as stated in the experimental section). Fe(II) content in the column influent was fixed at 1.79×10^{-4} mol/L (or 10.0 ppm Fe). The time-dependant removal efficiency of Fe(II) by brick grains (sizes : 0.7 - 1.0mm) is represented in Fig. 4a.

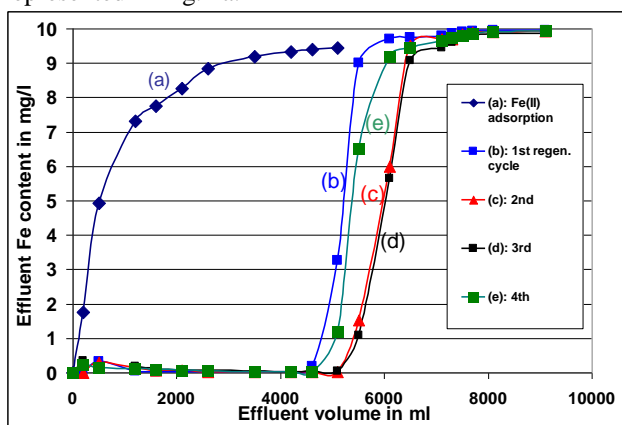Fig. 4: Breakthrough curves representing iron(II) adsorption on to: **(a)** 6MHCl - treated brick; and **(b)** after 1st; **(c)** 2nd; **(d)** 3rd; and **(e)** 4th column regeneration with NaClO. Flow rate: 10 mL/min; bed height: 8.5 cm; inside column diameter: 12.5 mm; influent Fe(II) concentration: 1.48×10^{-4} mole per liter.

As can been seen in this figure, the adsorption properties of 6M-HCl activated brick was found to be very weak. After exhaustion, the column regeneration was subsequently made for the elution of iron(II) (adsorbate) from aqueous solution by using a NaClO solution (8 g of chlorine per liter, and pH ≈ 11) under identical conditions of hydraulic loading rate (5 $ml.min^{-1}$). An oxidation reaction between the Fe(II) adsorbate and the ClO^- oxidant took place according to:

$$3H_2O + Na^+ClO^- + 2Fe^{2+} \rightarrow 2FeOOH + Cl^- Na^+ + 4H^+ \quad (2)$$
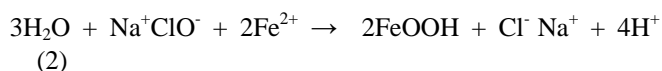
This reaction then brought about an additional amount of iron oxyhydroxide at brick surfaces, followed by the neutralization of hydroxyl functions bound to Si, Al and Fe atoms (represented by: ≡SOH). The influent solution of iron(II) (at a concentration of 1.79×10^{-4} mol/L) which was initially used in the first column experiment, was again passed through the column. Fig. 4b illustrates the breakthrough curve which was used to determine the

continuous flow adsorption capacity (Qe) for this modified brick. Our results showed clearly that the adsorption characteristics of the brick thus coated in the column were much better than those of 6M-HCl activated brick (see Fig. 5 and Table 1).
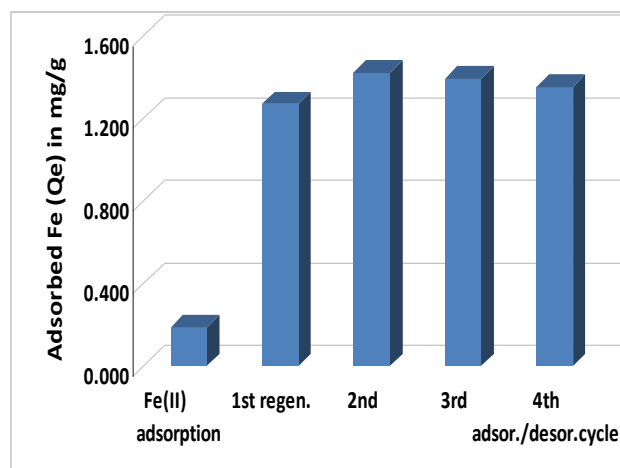

Fig. 5: Increasing amounts of iron (mmol/g) deposited on to brick grains (pre-treated with 6M HCl at 90°C for 3 hours) during four successive column regenerations with NaClO.

Table 1: Effect of NaClO regeneration on iron(II) adsorption capacity (Qe in mg/g) on to brick which was pre-treated with 6M HCl for 3 hours at 90°C.

|	Before regen.	1st After regen.	2nd ''	3rd ''	4th ''
Qe (mg/g)	0.18(8)	1.27(2)	1.42(3)	1.39(4)	1.35(5)

The formation of iron oxyhydroxide during the column regeneration therefore contributed to an increase of the adsorption capacity of the material used. To increase much more the quantity of iron oxihydroxide in the column, we decided to investigate successively up to four adsorption / desorption cycles under identical operation conditions. Our findings revealed clearly that the adsorption efficiency of the column gradually increased as the adsorption / desorption cycles continued up to n =2 and 3 (see Figs. 4c and 4d), owing to a FeOOH enrichment of the brick (see Figs. 5 and Table 1), thus confirming the importance of the iron oxyhydroxide phase in the promotion of cations adsorption. However, from the n = 4 regeneration cycle, the column efficiency tended to stabilize (see Figs. 4e and 5 and Table 1). This observation indicated that: (i) a large amount of iron oxyhydroxides amended to brick surface was not accessible for possible iron(II) adsorption due to layering; and (ii) probably a deactivation / depletion occurred in the column - packed material due to a disintegration of brick grains during adsorption / desorption cycles after repeated re-uses.

Moreover, in recent works by our research group [10, 11], we attempted to detect changes in the concentration of the specific ions: divalent metals ($Me^{2+}= Cd^{2+}$ or Fe^{2+}), and Na^+ and H^+ ions in the effluent during column experiments. The principal objective of these column studies was to know how

these entities interacted with the brick, and consequently, how they were implicated in the adsorption process. On the basis of findings, it was demonstrated clearly the predominant involvement of an ions-exchange reaction as:

$$2(\equiv SONa) + Me^{2+} \leftrightarrow (\equiv SO)_2Me + 2Na^+ \qquad (3)$$
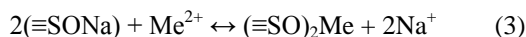
where "$\equiv SO$" represents reactive brick sites. To ensure electric (charge) balance, the exchange equilibrium between brick protons and Me^{2+} ions in water, as reaction (3), should further be taken into account:

$$2(\equiv SOH) + Me^{2+} \leftrightarrow (\equiv SO)_2Me + 2H^+ \qquad (4)$$
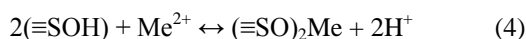
However, the implication of reaction (4) was found to be weak, and hence, the quantity of Na^+ ions released from the composite during the course of the column experiment could be roughly equated with the number of active sites present at the adsorbent surface. In this context, the knowledge of the amount of Na^+ ions bound to the brick might be considered as a good indicator for the appraising of the adsorption capacity of the different synthesized composites before their use as potential adsorbents for metal removal.

Taking into account this consideration, attempts were made in what follows to analyze reactive basic groups, $\equiv SO\text{-}Na^+$, in coated - brick by electrochemical techniques and to differentiate the types of basic functions present at the material surface.

D. Electrochemical studies

Potentiometric titrations of coated brick samples (0.7 -1.0 mm sizes) in water are presented in Fig. 6.
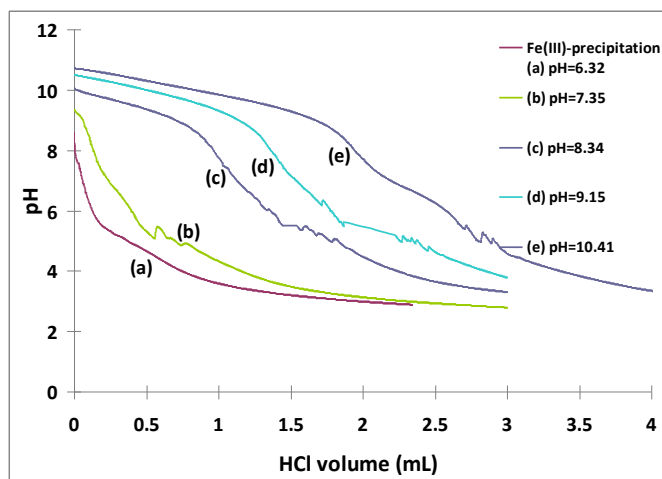

Fig. 6: pHmetric titration of different coated brick samples (0.5g of brick grains with 0.7 - 1.0 sizes), suspended in MilliQ water (90 mL) by means of a 0.05M HCl solution. Brick was coated with iron oxyhydroxide by precipitating Fe^{3+} ions with NaOH at the pH: **(a)** 6.32; **(b)** 7.35; **(c)** 8.34; **(d)** 9.15; **(e)** 10.41.

The addition of H^+ ions into modified brick resulted in the neutralization of basic functions: $\equiv SO\text{-}Na^+$. Substantial differences in titration behavior between the different titrated samples can be observed (Fig. 6). Thus, the quantity of H^+ ions necessary to neutralize all the $\equiv SO\text{-}Na^+$ groups anchored

in the brick surface, was found to increase with the Fe(III)-precipitation pH (which was initially fixed for coated-brick synthesis). From the different potentiometry curves obtained, the various amounts of reactive basic groups in brick grains (which were coated at different Fe(III)-precipitation pH ranging from 6.32 to 10.41), could then be assessed from the added volumes of titrated HCl solution at the inflection points. However, to ensure a better exploitation of these curves we preferred to examine the first derivative plot dpH/dV (y-axis) versus added HCl volume (x-axis), see Fig. 7.

As seen in this figure, at least two peaks could be detected for coated brick synthesized at Fe(III)-precipitation pH 10.4, b, thus revealing the relevance of Fe(III)-precipitation pH in coated-brick synthesis. This finding suggested that H^+ ions could be adsorbed on different types of (available) surface sites of the composite represented here by '$\equiv SO^-$'. From these potentiometric studies, it could be concluded that: (i) at precipitation pH < 7 roughly one peak was predominant and this peak represented mainly the acidification of the basic sites $\equiv FeO^-Na^+$, and certainly to a lesser extent that of the $\equiv SiO^-Na+$ sites; and (iii) at precipitation pH > 7 at least two peaks were observed, indicating the acidification of the basic sites $\equiv SiO^-Na^+$ and $\equiv AlO^-Na^+$ in addition to that of $\equiv FeO^-Na^+$.

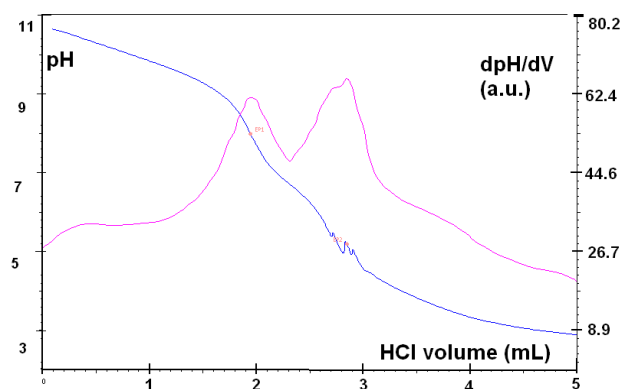Fig. 7: First derivative plot dpH/dV (y-axis) versus added H^+ species (x-axis), relative to the pHmetric titration of coated brick at pH 10.4 (0.5g of 0.7 - 1.0 sizes grains), suspended in MilliQ water (90 mL), with a 0.05 HCl solution.

Conductimetric titrations of brick grains (0.7 -1.0 mm sizes) coated with ferrihydrite at Fe(III)-precipitation pH 6.3, are presented in Fig. 8A.
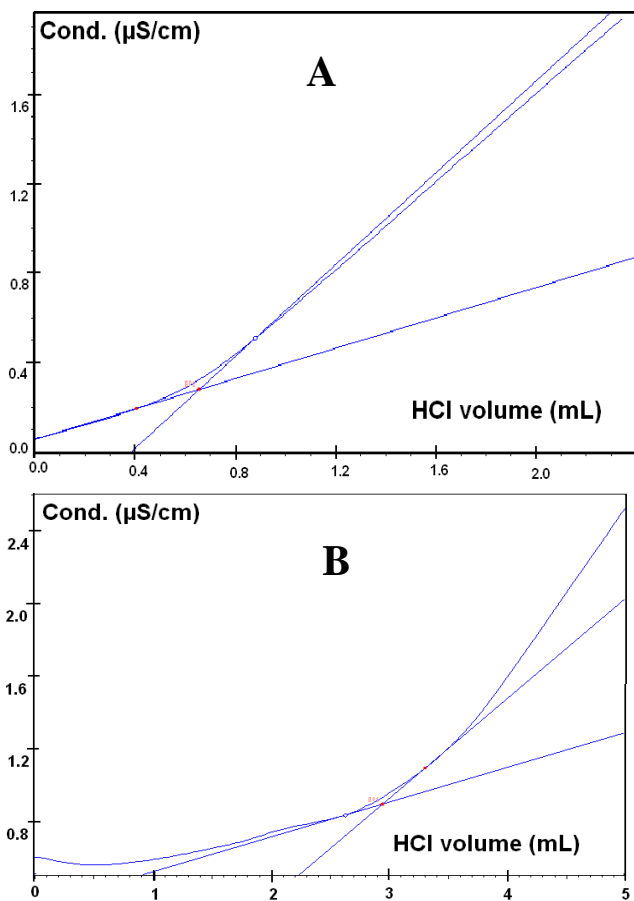
Fig. 8: Conductimetric titrations of brick grains (0.6-1.0 mm sizes) pre-coated with ferrihydrite at Fe(III)-precipitation pH: **(A)** 6.3; **(B)** 10.4. For that, 0.5 g of brick grains was suspended in 90 mL of MilliQ water.

As can be seen in this figure, the end of the acidification reaction between basic group $\equiv SO^-Na^+$ and added H^+ ions can be easily detected at the inflection point. It could further be noticed in Fig. 8A that an abrupt change of conductivity appeared in the titration curve after brick acidification when H_3O^+ ions became in excess. This phenomenon was due to the high equivalent - limit conductivity value for H_3O^+ ions in water (λ_{H3O^+} = 34.96 mS.m².mol⁻¹ [20]), when compared to that for Na^+ ions (λ_{Na+}=_5.01_mS.m².mol⁻¹ [20]). This observation showed clearly the labile characteristics of sodium ions bound to the various ligands belonged to the activated brick, in agreement with the ^{23}Na NMR observations confirming the existence of outer – sphere complexes implicating hydrated sodium ions, $Na(H_2O)_n^+$, water molecules and active brick sites [11]. As for the brick coated with FeOOH at higher Fe(III) – precipitation pH values (*e.g.*, pH 10.4), the conductimetric - titration curve arising from the addition of H^+ ions exhibits one inflection point (Fig. 8B). It can however be noticed that one inflection point (not interpreted) was barely detected at the beginning of the process. The volumes of H^+ ions solution added into the suspension permitted us to evaluate the amounts of these basic groups in the brick. These quantities as well as those of Na and Fe atoms determined by ICP-AES are listed in Table 2.

Table 2: ICP-AES results on Fe and Na amounts in the brick pre-coated at different Fe(III)-precipitation pH values, and potentiometry data on their acid-base characteristics.

(pH$_{preci.}$): the pH value at which iron(III) was precipitated on to brick surfaces.

V_{E1} and V_{E2}: the HCl volumes determined at the two equivalence points in the pHmetric curve (for that, the first derivative plot (dpH/dV (y-axis) versus added H^+ species (x-axis)) was used, see Fig. 7).

pH$_{E1}$ and pH$_{E2}$: the pH values at the two equivalence points.

m$_{brick}$: the mass of coated brick, suspended in 90 ml of milli-Q water, used for pHmetric titration.

V$_{conduc.}$: the HCl volume added to the suspension in order to neutralize hydroxyl groups in the brick, and determined by conductimetry.

[ΞSO^-]$_{tot}$: the total quantity of basic sites evaluated by potentiometry.

[Na]: the amount of brick sodium determined by ICP-AES.

[Fe]$_{deposited}$: the total quantity of iron deposited on to the brick surface at a fixed pH by Fe(III) precipitation with NaOH, and determined using ICP-AES.

Coated brick (pH$_{preci.}$)	m$_{brick}$ /g	pH$_{E1}$	V$_{E1}$ /ml	pH$_{E2}$	V$_{E2}$ /ml	V$_{conduc.}$ /ml	[ΞSO^-]$_{tot.}$ /(mmol/g)	[Na] /(mmol/g)	[Fe]$_{deposited}$ /(mmol/g)
(6.32)	0.510	7.43	0.036	4.49	0.550	0.601	0.059	0.084	0.083
(7.35)	0.502	7.90	0.140	4.70	0.842	0.846	0.085	0.138	0.080
(8.34)	0.561	7.80	0.991	5.51	1.453	1.453	0.130	0.167	0.078
(9.15)	0.540	7.65	1.380	5.36	2.030	2.048	0.190	0.206	0.091
(10.41)	0.461	7.98	1.945	5.19	2.847	2.940	0.320	0.434	0.089

It should be noted that the amount of basic groups found in the brick coated at pH 6.3 equated well that of iron deposited on to this material, suggesting that Na atoms were preferentially bound to the iron - oxyhydroxide phase as "$\equiv$FeOONa". In contrast, for the brick coated at pH > 7 sodium contents tended to increase significantly, while iron contents remained nearly constant. This indicated that Na^+ ions were further bound to other basic sites like silanol and aluminol in brick aluminosilicates which were mainly originated from hydroxylated metakaolinite.

Moreover, from these electrochemical studies it had been possible to evaluate the total quantity of basic groups in the different synthesized composites. We found [$\equiv SO^-$] varying from 0.059 to 0.320 mmol per gram of brick (see Table 2). And the number of active sites at the brick surface ranged from 5.07×10^{16} to 2.75×10^{17} per gram of material.

In an attempt to quantify the surface chemistry of these coated bricks, pHmetric titrations with a 0.05M HCl solution were performed on two brick samples (which were initially pre-activated with 6M HCl at T=90°C for 3 hours): (i) one neutralyzed by NaOH at a fixed pH ~11; and (ii) the other coated with iron oxyhydroxide at pH 7.2 and followed by a NaOH leaching of the material at pH ~11. Each of these titrations lasted more than two days. The pHmetric analysis of the first sample (see Fig. 9A) enables the observation of brick protons and determination of their consumption from aluminosilicate surfaces, *i.e.* ΞSiO^- and ΞAlO^- sites. While the pHmetric analysis of the second sample (see Fig. 9B) permits in addition the detection and evaluation of protons

consumption from iron - oxyhydroxide surfaces. The first derivative plots dpH/dV (y-axis) versus added HCl volume (x-axis) show clearly the occurrence of two equivalence peaks in Fig. 9A and three peaks in Fig. 9B.
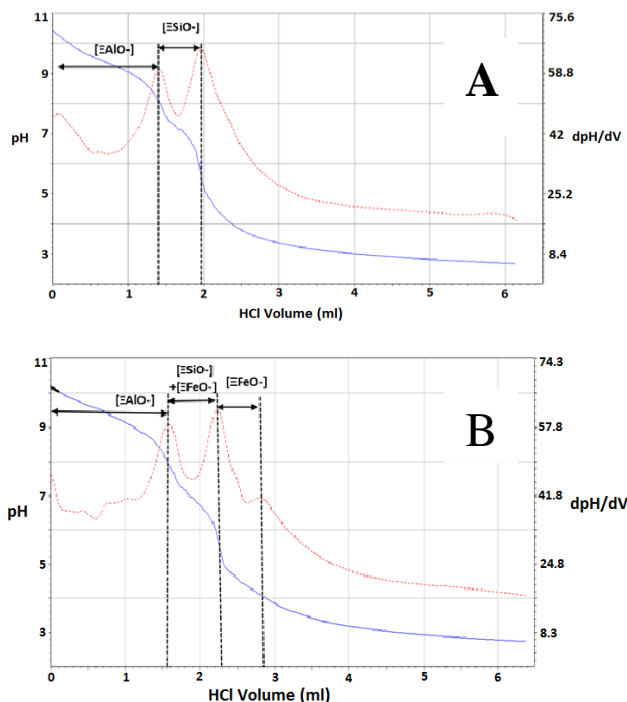

Fig. 9: pHmetric titrations with a 0.05M HCl solution performed on two brick samples which were prepared as follows: **(A)** raw brick pre-activated with 6M HCl at T=90°C for 3 hours and neutralyzed by NaOH at a fixed pH ~11; and **(B)** brick first 6M HCl pre-activated, second coated with iron oxyhydroxide at pH 7.2 followed by a NaOH leaching of the material at pH ~11.

In agreement with acid/base characteristics of aluminol and silanol generally found in aluminosilicates (see Fig. 2), H^+ ions are found to be preferentially consumed by ΞAlO^- sites at pH ranging from 7.8 to 10.5, while preferentially consumed by both ΞSiO^- and ΞFeO^- sites at pH from 5.6 to 7.8, and finally by weaker (different) basic ΞFeO^- sites at pH < 5.6. Note, however, that in order to interpret protons consumption by the brick in water, we hypothesized that at least two basic forms of ΞFeO^- species should exist at the brick surface. Indeed, in a recent paper we reported the existence of (Al, Si, Fe, O) combinations/ clusters which were generated during the adsorbent synthesis through iron(III) precipitation with NaOH at the brick surface [21].

To better understand the enhancing adsorption capacity of modified brick in metal removal from water, it was necessary to know the extent to which *first* the pore – size distributions of synthesized coated bricks and *second* their chemical surface characteristics, affected the adsorption process.

E. Parameter(s) controlling adsorption process

E-a Physical / textural modifications at the coated brick surface

Figure 10 illustrates the evolution of the pore size distribution of FeOOH - coated brick synthesized at different Fe(III)-precipitation pH values ranging from 6.3 to 12.9.
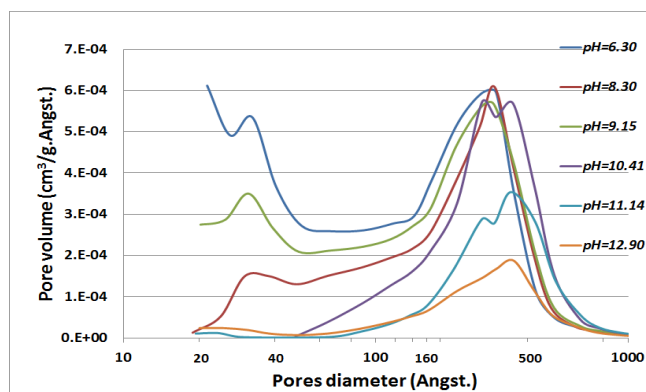

Fig. 10: Evolution of the pore - size distribution of brick grains (0.7 – 1.0 mm sizes) when pre-coated them with iron oxyhydroxide at different Fe(III)-precipitation pH values ranging from 6.3 to 12.9.

Pore size distributions of FeOOH - coated brick grains (0.7 – 1.0 mm sizes) show that roughly two types of pores predominate in this material: mainly pores with diameters ranging from ~20 Å to ~40 Å. The highest volume of mesopores (centered at about 30 Å) was observed in the brick which was previously coated at precipitation pH 6.3. In addition, it was demonstrated that: (i) as the precipitation pH increased, the volume of these mesopores (with pores diameter: ~30 Å) decreased dramatically at the brick surface, and became even negligible at pH > 10; (ii) the peak intensity relative to macropores with an averaged diameter of ~300 Å remained relatively constant up to pH 10.41, and decreased significantly at higher pH values; and (iii) while at pH ≥10.4 a new peak of macropores appeared at around 400Å, see Fig.10. However, the population of these macropores (with diameters ~ 400Å) was found to decrease rapidly on brick surfaces when these were impregnated with iron oxyhydroxides at precipitation-pH values 11.14 and 12.90, see Fig. 10. This phenomenon could be due to a progressive textural degradation of the material in basic media, in agreement with microscopic (SEM) analyses performed on our samples (not shown here).

When compared to HCl - activated brick grains (0.7 – 1.0 mm sizes), the deposition of ferrihydrite on to this material at pH 6.3 contributed to a decrease of the surface area (S.A.) from 75.5 to 58.2 m^2/g and the mesopores volume (V_{pore}) from 0.21 to 0.18 cm^3/g. And, after increasing the Fe(III) - precipitation pH from 6.3 to 12.9 for the coating of the brick with FeOOH, the V_{pore} value was found to decrease from 0.179 to 0.06 cm^3/g (Fig. 11A and Table 3), and the S.A. value from 58.5 to 8.2 m^2/g (Fig. 11B and Table 3).

Table 3: Pore-size distribution data obtained for brick grains (0.7 – 1.0 mm sizes) when pre-coated with iron oxyhydroxide at different Fe(III)-precipitation pH values ranging from 6.3 to 12.9. V_{pore} with diameters varying from 17 to 1000 Å.

	FeOOH-COATED BRICK (pH$_{preci.}$)					
pH	(6.3)	(8.3)	(9.1)	(10.4)	(11.1)	(12.9)
S.A. m^2/g	58.5	46.5	40.22	22.7	13.5	8.2
V$_{pore}$ cm^3/g	0.179	0.155	0.177	0.176	0.115	0.058
Averaged pore, Φ (Angst.)	114	210	155	250	257	231

In addition, the specific surface area was found to decrease with an increasing amount of sodium fixed at the brick surface during the FeOOH – coating procedure (Fig. 11B). To summarize, the detailed examination of specific surface areas (S.A.) and pore volumes (V$_{pore}$) of brick composites allowed us to reveal two main facts: (i) the high values of these parameters (S.A. and V$_{pore}$) obtained initially for HCl-activated brick favored rather the fixation of iron oxyhydroxide on to the brick surface; and (ii) the textural and morphological properties of the resulting 'coated' material (after FeOOH coating at various Fe(III)-precipitation pH) did not intervene as key factors in the adsorption mechanism
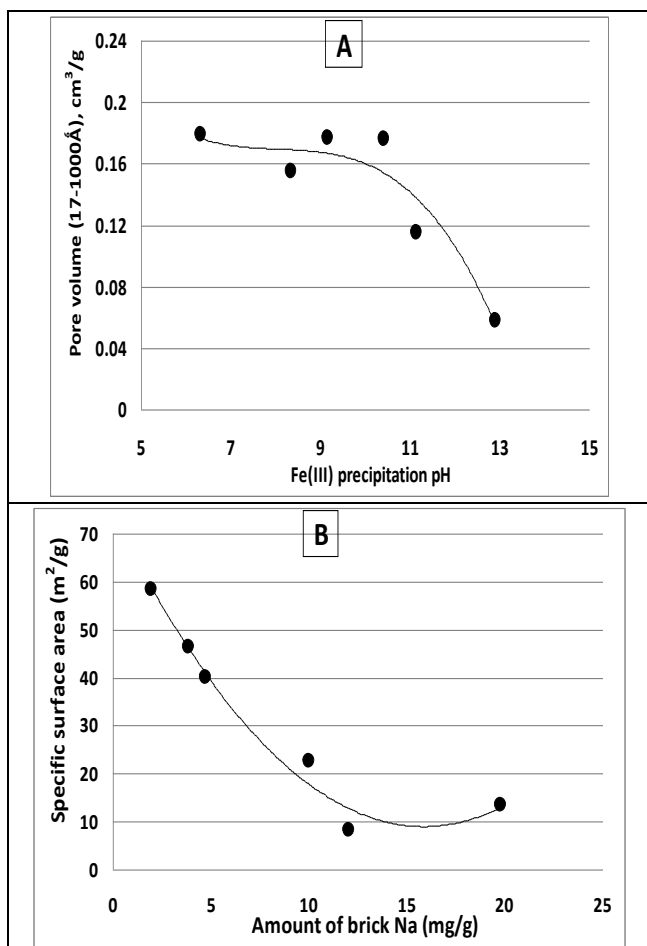

Fig. 11: **(A)** Pore volume (17-1000 Å; cm^3/g) plotted against Fe(III)-precipitation pH. **(B)** Specific surface area (m^2/g) plotted against the amount of brick Na (mg/g).

.
Consequently, BET data about pore-size distributions could not explain directly the extent of adsorption capacities

measured for the different composites when these were used as adsorbents in fixed-bed column.

E-b Chemical modifications at the coated brick surface

In section 3.2, we examined the adsorption behavior of Pb^{2+} in a fixed bed of two kinds of brick grains: one impregnated with iron oxyhydroxides at Fe(III) - precipitation pH = 6.3; and the other at Fe(III) - precipitation pH = 10.4. The molecular quantities of Pb(II) adsorbed on to the brick were determined by integrating the breakthrough curves illustrated in Fig. 3, and these values were compared to the molecular contents of sodium released in the influent. We found [Na] ≈ 2 [Pb]. As suggested previously [9], the Pb(II) - adsorption occurred simply according to the ions-exchange reaction:

$$2(\equiv SONa) + Pb^{2+} \leftrightarrow (\equiv SO)_2Pb + 2Na^+ \qquad (5)$$
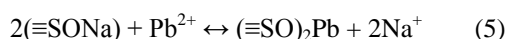
Pb^{2+} adsorption then led to the formation of an inner - sphere bidendate complexe [9].
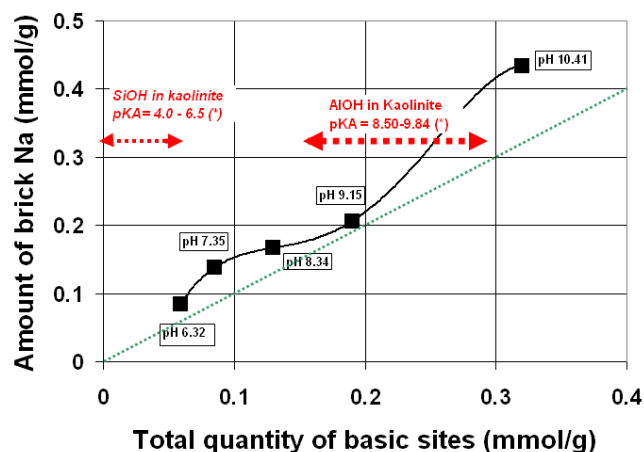

Fig. 12: Variation of brick-Na amount (determined using ICP-AES) as a function of the total quantity of basic sites (determined by pHmetry) in the various coated bricks. (*) see ref. 22.

Moreover, the adsorption capacity of the composite prepared at pH 10.4 was found to be 3.7 times higher than that of the synthesized at pH 6.3, suggesting that the number of basic groups, represented as ≡SO$^-$Na$^+$, could be a key factor controlling the adsorption capacity level in the brick medium. In this assumption, the ratio Q$_{ads(pH\ 10.4)}$/Q$_{ads(pH\ 6.3)}$ was compared to that of Na contents which were determined by ICP-AES for coated bricks prepared at the same Fe(III) – precipitation pH values:

$$\frac{Q_{ads(pH=10.4)}}{Q_{ads(pH=6.3)}} = 3.7 < \frac{[Na]_{(pH=10.4)}}{[Na]_{(pH=6.3)}} = 5.17$$

The ratio Q$_{ads(pH\ 10.4)}$/Q$_{ads(pH\ 6.3)}$ was also compared to that of basic sites, **"S"** which were determined by pHmetry:

$$\frac{Q_{ads(pH=10.4)}}{Q_{ads(pH=6.3)}} = 3.7 < \frac{[S]_{(pH=10.4)}}{[S]_{(pH=6.3)}} = 5.42$$

The curve representing the evolution of brick-Na amount versus basic-sites content (Fig. 12) revealed a discrepancy due to an excess of sodium with regard to $\equiv SO^-$ groups: indeed, all the experimental points shown in Fig. 12 are situated above the bisector drawn in dashed line.

All these discrepancies could be explained partly by the no-reactivity of certain hydroxyl groups at the brick surface towards Pb^{2+} ions probably because of the weakly basic properties of some $\equiv SiO^-$ sites or highly acidic behavior of corresponding silanols. This suggestion is consistent with relatively weak acid/base characteristics of silanols in kaolinite [22], which is a structurally ordered aluminosilicate and also (chemically) enough comparable with hydroxylated metakaolinite (despite its disordered structure) present in the brick framework. Indeed, in comparison with the pK_A values for surface dissociations of silica and alumina in kaolinite (as illustrated in Figs. 2 and 12), it might be deduced that in the aluminosilicates phase of the brick the first (easiest) deprotonation should take place at Si sites, while the second would occur at Al sites, as displayed in Figs. 2 and 12. As for iron-oxyhydroxide deposited on to brick, their surface undergoes deprotonations progressively with Si sites and this process ends well before starting deprotonations of Al sites, as shown in Figs 2 and 12. It is however important to note that, as illustrated in Fig. 12, the excess of sodium found in coated brick detected by ICP-AES analysis (with reference to basic "$\equiv SO^-$"functions determined by potentiometry) might certainly result from the formation of complex associations between Na-aluminosilicates and ferrihydrite [21], leading in part to (Si, Al)-bearing ferrihydrites as already pointed out by Cismura and her coworkers [23-25]. Heterogeneous (Si, Al, Fe) combinations/clusters with variable compositions then raise the possibility of Fe-contained brick surfaces with basic characteristics that differ from those of pure FeOOH and should be not or partly affected by HCl reagent during pHmetric titration

IV. CONCLUSION

From this study, we have identified a low cost and efficient activation procedure for enhancing the adsorption capacity of brick. The deposition of iron oxyhydroxide on to HCl-leached brick was made at different Fe(III)-precipitation pH. It was noticed that an increase of this pH resulted in higher levels of sodium bound to the material. The existence of these Na atoms was found to be intimately related to the generation of basic (negatively charged) sites at the brick surface. Electrochemical studies permitted us to quantify basic groups present on coated - brick and to differentiate the types of basic functions present at the material surface. Fixed-bed column studies allowed us to determine the adsorption capacity of coated brick in the removal of lead(II) and iron(II) from water. Column regeneration with NaClO as an eluent was preferred for two reasons: (i) as a means to increase the amount of iron at the brick surface and (ii) to create fresh reaction sites for subsequent Fe(II) adsorption. The number of generated basic groups was a key factor controlling the adsorption capacity level in the brick medium.

However, some of these sites were found to be not reactive because of their weakly basic properties towards Pb^{2+} ions. The number of reactive sites involved in each of column experiments was compared with those of Na atoms and basic sites determined by ICP-AES and pHmetry, respectively. The discrepancies found were related to acid / base properties of silanols and perhaps due as well to the existence of stable (Al, Si, and/or Fe) combinations at the brick surface. Overall, chemical surface modifications applied in this work to the brick contributed to improve significantly adsorption process. Conversely, parameters relative to structural and textural changes on the brick seemed not to control adsorption mechanism.

REFERENCES

[1] V.K. Gupta, I. Ali, Water treatment for inorganic pollutants by adsorption technology, Environmental Water (2013) 29-91.

[2] U. Schwertmann, R.M. Cornell, Iron oxides in the Laboratory : Preparation and Characterization, VCH Publishers, New York, 1991.

[3] L.C.A. Oliveiraa, R.V.R.A. Riosa, J.D. Fabrisa, K. Sapagb, V.K. Gargc, R.M. Lagoa, Clay-iron oxide magnetic composites for the adsorption of contaminants in water, Appl. Clay Sci. 22 (2003) 169–177.

[4] L.C.A. Oliveiraa, D.I. Petkowiczb, A. Smaniottob, S.B.C. Pergher, Magnetic zeolites: a new adsorbent for removal of metallic contaminants from water, Water Res. 38 (2004) 3699–3704.

[5] R.L. Vaughan Jr., B.E. Reed, Modeling As(V) removal by a iron oxide impregnated activated carbon using the surface complexation approach, Water Res. 39 (2005) 1005–1014.

[6] F. Unob, B. Wongsiri, N. Phaeon, M. Puanngam, J. Shiowatana, Reuse of waste silica as adsorbent for metal removal by iron oxide modification, J. Hazard. Mat. 142 (2007) 455-462.

[7] T. Phuengprasop, J. Sittiwong, F. Unob, Removal of heavy metal ions by iron oxide coated sewage sludge, J. Hazard. Mat. 186 (2011) 502-507.

[8] A. Eisazadeh, H. Eisazadeh, K.A. Kassim, Removal of Pb(II) using polyaniline composites and iron oxide coated natural sand and clay from aqueous solution, Synthetic Metals 171 (2013) 56-61.

[9] S.C. Dehou, M. Wartel, P. Recourt, B. Revel, J. Mabingui, A. Montiel, A. Boughriet, Physicochemical, crystalline and morphological characteristics of bricks used for ground waters purification in Bangui region(Central African Republic), Applied Clay Science 59-60 (2012) 69-75.

[10] O. Allahdin, S.C. Dehou, M. Wartel, P. Recourt, M. Trentesaux, J. Mabingui, , A. Boughriet, Performance of FeOOH-brick based composite for Fe(II) removal from water in fixed bed column and mechanistic aspects, Chem. Eng. Res. Design 91 (2013) 2732-3742.

[11] O. Allahdin, , M. Wartel, P. Recourt, B. Revel, B. Ouddane, G. Billon, J. Mabingui, , A. Boughriet, Adsorption capacity of iron oxihydroxide-coated

brick for cationic metals and nature of ion surface interactions, Appl. Clay Sci. 90 (2014) 141-149.

[12] M.C. Reiley, Science, policy, and trends of metals risk assessment at EPA: How understanding metals bioavailability has changed metals risk assessment at USEPA, Aquat. Toxicol. 84 (2007) 292–298.

[13] A. Fairbrother, R. Wenstel, K. Sappington, W. Wood, Framework for metals risk assessment, Ecotoxicol. Environ. Saf. 68 (2007) 145–227.

[14] USEPA (2002). National Recommended Water Quality Criteria: 2002. Office of Water, Washington, DC.

[15] A. Pagliuca, G.J. Mufti, D. Baldwin, A.N. Lestas, R.M. Wallis, A.J. Bellingham, Lead poisoning: clinical, biochemical, and haematological aspects of a recent outbreak, J. Clin. Pathol. 43(4) (1990) 277-281.

[16] WHO(1993). Guidelines for drinking water quality. In: Recommendations, second ed. Vol.1 World Health Organization. Geneva. Switzerland.

[17] P. Mushak, Lead remediation and changes in human lead exposure: some physiological and biokinetic dimensions, The Science of the Total Environment 303 (2003) 35-50.

[18] A. Azizullah, M. N. K. Khattak, P. Richter, D.P. Hader, Water pollution in Pakistan and its impact on public health—a review, Environ. International 37 (2011) 479-497.

[19] S. Khan, M. Shahnaz, N. Jehan, S. Rehman, M. T. Shah, Drinking water quality and human risk in Charsadda district, Pakistan, Journal of Cleaner Production 60 (2013) 93-101.

[20] F. Miomandre, S. Sadki, P. Audebert, R. Méallet-Renault (2005), Electrochimie : Des Concepts aux Applications, Science Sup.,Dunod, Paris.

[21] O. Allahdin, M.Wartel, J. Mabingui, B. Revel, N. Nuns, A. Boughriet, Surface characteristics of the iron-oxyhydroxide layer formed during brick coatings by ESEM/EDS, 23Na and 1H MAS NMR, and ToF-SIMS, Material Chemistry and Physics 165 (2015),215-226.

[22] F.J. Huertas, L. Chou, R. Wollast, Mechanism of Kaolinite Dissolution at Room Temperature and Pressure: Part 1. Surface Speciation, Geochimica et Cosmochimica Acta 62 (1998) 417-431.

[23] A. C. Cismasu, F. Marc Michel, J. F. Stebbins, C. Levard , G. E. Brown Jr., Properties of impurity-bearing ferrihydrite I. Effects of Al content and precipitation rate on the structure of 2-line ferrihydrite, Geochimica et Cosmochimica Acta 92 (2012) 275–291.

[24] A.C. Cismasu, C. Levard, F.M. Michel, G. E. Brown Jr., Properties of impurity-bearing ferrihydrite II: Insights into the surface structure and composition of pure, Al- and Si-bearing ferrihydrite from Zn(II) sorption experiments and Zn K-edge X-ray absorption spectroscopy, Geochimica et Cosmochimica Acta 119 (2013) 46-60.

[25] A.C. Cismasu, F.M. Michel, A.P. Tcaciuc, G. E. Brown Jr., Properties of impurity-bearing ferrihydrite III. Effects of Si on the structure of 2-line ferrihydrite, Geochimica et Cosmochimica Acta 133 (2014) 168-185.